

## ELECTROCHEMICAL INSERTION OF LITHIUM IN MANGANESE DIOXIDE

JIRÍ VONDRÁK, IVO JAKUBEC and JANA BLUDSKÁ

*Institute of Inorganic Chemistry, Czechoslovak Academy of Sciences, Majakovského 24, 160 00 Prague 6 (Czechoslovakia)*

### Summary

The insertion of lithium into compact electrolytic  $\text{MnO}_2$  was studied by galvanostatic and admittance techniques. The diffusion coefficient,  $3.4 \times 10^{-14} \text{ m}^2/\text{s}$  at  $20^\circ\text{C}$ , and its activation energy of 30 kJ were determined. The rate of the process is controlled mainly by the high resistivity of  $\text{MnO}_2$  and by the polarization of the electrode reaction itself. Similarly, the behaviour of  $\text{MnO}_2\text{-C}$  plastic bonded electrodes is controlled mainly by the high resistivity of  $\text{MnO}_2$  if the content of carbon black is not sufficient to form a conductive network, and by polarization on the grains of  $\text{MnO}_2$  at higher carbon black contents. The optimum concentration of carbon is 30 - 40% by volume.

---

### Introduction

Many papers [1 - 3, 11] have been published on the insertion of lithium in  $\text{MnO}_2$ . This process has been studied on a plastic bonded powder of  $\gamma\text{-MnO}_2$  and carbonaceous material. It occurs in the potential range 3.05 - 2.85 V vs.  $\text{Li}/\text{Li}^+$  and it is partially reversible [2, 4]. The aim of this paper is to investigate this process on electrolytically manufactured compact  $\text{MnO}_2$  and an attempt will be made to compare the results obtained with the properties of plastic-bonded  $\text{MnO}_2$  cathodes.

### Experimental

Compact electrolytic  $\text{MnO}_2$  was cut into chips 0.5 - 3 mm thick. One side of each was coated with sputtered gold and then electroplated with copper, and a wire was soldered to the copper layer. The electrode was sealed in a glass tube using epoxy resin.

Battery-grade  $\gamma\text{-MnO}_2$  (Knapsack GmbH, BDR) and carbon black CORAX 5 HS (Deutsche Gasrusswerke GmbH, Dortmund, BDR) were thoroughly mixed and the PTFE suspension Fluon (Imperial Chemical Industries, Ltd., U.K.) was added until the mixture attained the consistency of a dough;

the blend was dried and deposited on a nickel screen, wrapped in aluminium foil and pressed. The screen of apparent area  $1 \text{ cm}^2$  was then mounted by a platinum screw onto a PTFE holder.

A three-electrode cell and 1.0M  $\text{LiClO}_4$  in propylene carbonate were used for all experiments. Potentials are referred to a lithium reference electrode.

Galvanostatic curves were measured in the usual way with prepolarization by means of a potentiostat or without it. A Solartron 1250 Signal Analyzer with a Solartron 1841 Electrochemical Interface was used for admittance measurements.

Electrical properties were measured on pellets pressed from blends of  $\text{MnO}_2$  with carbon black; the resistivity was measured under constant pressure (approx. 70 kPA), and the thermoelectric power was measured in a device described earlier [5].

## Results and discussion

### (A) Compact $\text{MnO}_2$

Several galvanostatic curves can be successfully observed on a single electrode if the electrode is polarized, between successive experiments to 3.3 - 3.4 V. In Fig. 1, the potential is plotted against the product  $i \times t^{1/2}$  for several current densities. From the results it follows:

(i) The transition time,  $\tau$ , is inversely proportional to the square of the current density,  $i$ . Therefore, the insertion of lithium is limited by diffusion; on the assumption that  $\text{Li}_{1.0}\text{MnO}_2$  is formed in a single-phase reaction [3],

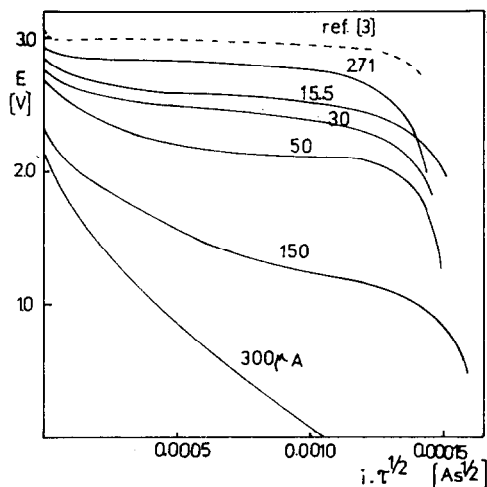


Fig. 1. Galvanostatic curves of lithium insertion into compact  $\text{MnO}_2$  at various currents in 1M  $\text{LiClO}_4/\text{PC}$  electrolyte. - - -, equilibrium according to ref. 3. Electrode area  $5 \text{ mm}^2$ .

the diffusion coefficient  $D = 3.4 \times 10^{-14} \text{ m}^2/\text{s}$  was evaluated from the average value of the product  $i \times \tau^{1/2}$  ( $0.0290 \pm 0.0032$ ) using the Sand equation.

(ii) The beginning of all curves is shifted towards more negative potentials in proportion to the applied current. The resistance of the electrode,  $48 \pm 7 \text{ k}\Omega$ , was evaluated from this shift; the thickness of the electrode was about 2 mm and its surface area  $0.05 \text{ cm}^2$ .

(iii) The slope of the curves is higher for higher currents, indicating the occurrence of some polarization, which is increased by lithium enrichment of the electrode.

The admittance, plotted in a complex plane, is indicated in Fig. 2, in which the equivalent circuit is also shown. It consists of 7 components, which were found by means of extrapolation to infinite frequencies by a program on an H & P 9830 calculator in the interactive mode. The following conclusions can be drawn from the evaluated components:

(i) The resistance of the electrolyte,  $R_1$ , is approximately  $100 \Omega$ .

(ii) The capacity,  $C_1$ , is in the range 30 - 80 nF for an electrode surface of  $0.08 \text{ cm}^2$ ; most probably, it is the capacity of some barrier layer of a semiconductive nature.

(iii) The resistance  $R_2$  is the volume resistance of the electrode; its value at  $20^\circ \text{C}$  ( $1.9 \text{ k}\Omega$ ) and the dimensions of the sample ( $0.08 \text{ cm}^2 \times 0.5 \text{ cm}$ ) yield a specific resistivity of  $30.4 \Omega \text{ m}$ . The activation energy,  $2.69 \text{ kJ}$  ( $0.027 \text{ eV}$ ), was obtained from its dependence on temperature.

(iv) The admittance,  $W_1$ , has a phase shift of  $45^\circ$  and is proportional to  $(\omega \times C_1/R_2)^{1/2}$ ; therefore it is the admittance of fissures in the electrode seal or of pores in the electrode, which should behave as an infinite  $R$ - $C$  line.

(v) The interfacial capacity  $C_2$  is approximately  $100 - 200 \mu\text{F}/\text{cm}^2$ .

(vi) The resistance  $R_3$  is the true polarization resistance of the intercalation process; at  $20^\circ \text{C}$ , 3.0 V, and  $0.08 \text{ cm}^2$  electrode surface, its value is  $260 \Omega$  and its activation enthalpy is  $20.6 \text{ kJ}$ . Its value increases slightly with decrease of potential.

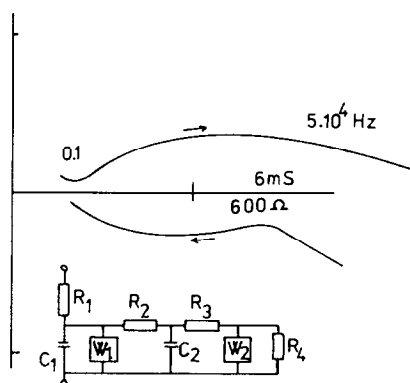


Fig. 2. Admittance (upper curve) and impedance (lower curve) of compact  $\text{MnO}_2$  electrode in the frequency range between 0.1 and 50 000 Hz. Electrode area  $8.05 \text{ mm}^2$ .

(vii) The diffusion admittance,  $W_2$ , passes through a maximum 18.3  $\text{mS Hz}^{-1/2}$  at 2.95 - 2.85 V. At 3.0 V it falls to 1.205  $\text{mS Hz}^{-1/2}$ . Using these data in the classical formula [6, 7] a diffusion coefficient,  $D = 1.2 \times 10^{-16} \text{ m}^2/\text{s}$  has been evaluated. However, the agreement with galvanostatic measurements would be better if the proper value of  $\partial E/\partial C_{\text{Li}}$ , the activity coefficient  $\gamma_{\text{Li}}$  of lithium in  $\text{MnO}_2$  and related quantities were available [8].

(viii) The activation energy of diffusion is quite high (30.3 kJ). Therefore, the lithium insertion diffusion control is a true, solid-state diffusion rather than the diffusion of lithium ions,  $\text{Li}^+$ , in the electrolyte contained in pores present, or perhaps created, in the electrode material [13 - 15]. Moreover, the admittance attached to the diffusion in the electrolyte in a porous electrode should be proportional to  $\omega^{1/4}$  and its phase angle should be  $22.5^\circ$  rather than  $45^\circ$ .

### (B) Electrical properties of $\text{MnO}_2$ -C mixtures

The apparent specific conductivity,  $\kappa$ , and the thermoelectric power,  $\alpha$ , are shown in Fig. 3. Essentially, the mixtures can be divided into two subgroups according to their properties and the carbon concentration.

(i) In range I (up to 30% C by volume), the conductivity is low and the properties gradually differ from those of compact  $\text{MnO}_2$ . It is considered that the grains of  $\text{MnO}_2$  are in contact with each other. The carbonaceous material fills the free space between the grains of  $\text{MnO}_2$  and forms continuous short-circuits and bridges.

(ii) In range II (over 30% C by volume), the carbon bridges fill the free space completely and form a continuous conductive network which provides contact with all the grains of  $\text{MnO}_2$ ; the electrical properties are quite close to those of pure carbon.

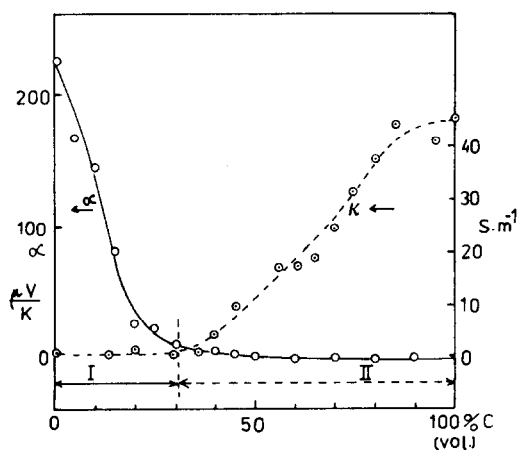


Fig. 3. The influence of carbon black content (in vol.%) on the thermoelectric power,  $\alpha$ , and the electrical conductivity,  $\kappa$ , of  $\text{MnO}_2$ -C mixtures.

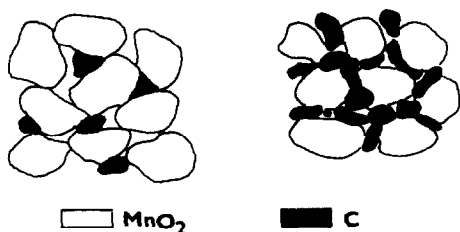


Fig. 4. Idealized view of  $\text{MnO}_2$  blends. Left: concentration of carbon lower than 25%, right: concentration higher than 25% (by volume).

Figure 4 shows an idealized view of blends of  $\text{MnO}_2$  and C of both concentration ranges.

### (C) Electrochemical properties of $\text{MnO}_2$ -C mixtures

Usually two waves appear on the cathodic galvanostatic curves of  $\text{MnO}_2$ -C mixtures (see Fig. 5). The wave of lithium insertion is in the expected potential range (3.1 - 2.2 V according to current density) and it is followed by a second wave starting at 1.6 V, at which lithium is inserted in carbon black and propylene carbonate is reduced [9, 10]. This wave is less pronounced on blends of low C content.

The coefficient of  $\text{MnO}_2$  utilization,  $K$ , depends both on applied current and composition, as Fig. 6 shows. For mixtures from range I it is approximately proportional to the conductivity of the blend (*cf.* Fig. 3), while it passes through a maximum at the lower end of range II, *i.e.*, for

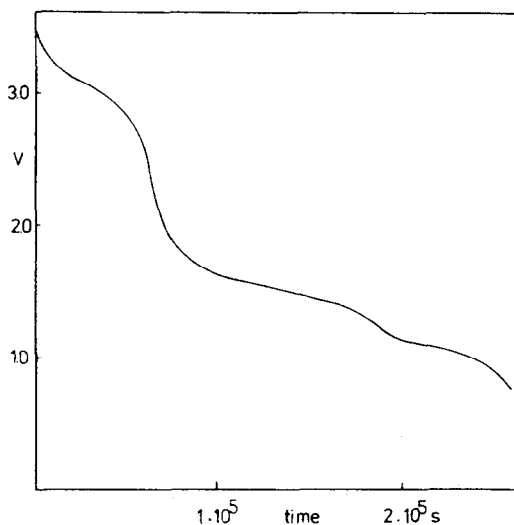


Fig. 5. Example of an electrode discharge containing 50% C by volume, 0.03 g by weight, at a current of 0.1 mA.

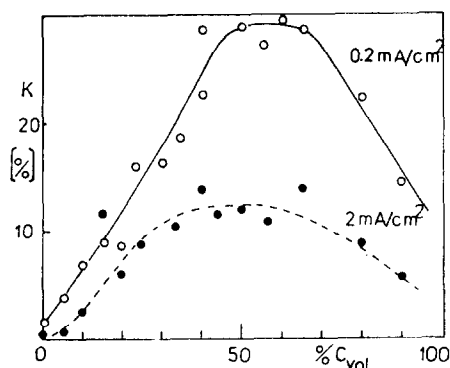


Fig. 6. The coefficient of  $\text{MnO}_2$  utilization,  $K$ , at 0.2 and 2.0  $\text{mA/cm}^2$ .

carbon contents of 40 - 50% by volume. At the highest carbon content,  $K$  decreases markedly; this can be explained by the increase in the true current density on the  $\text{MnO}_2$  grains in blends with a low  $\text{MnO}_2$  content, resulting in a higher influence of electrochemical overvoltage.

## Conclusions

The diffusion coefficient of lithium in  $\text{MnO}_2$  is fairly high ( $D = 10^{-14}$   $\text{m}^2/\text{s}$ ), apparently due to the tunnel structure of  $\text{MnO}_2$ , and connected with a higher coordination saturation of oxygen ions in such structures than in layered structures [12]. However, the influence of high electrical resistivity and, under certain circumstances, also of polarization effects, predominates and diffusion control can be observed only under certain conditions, both on compact and powdered electrodes. Hence, the diffusion of lithium in  $\text{MnO}_2$  is sufficiently rapid and does not strongly influence the behaviour of Li- $\text{MnO}_2$  cells.

## References

- 1 H. Ikeda, in J. P. Gabano (ed.), *Lithium Batteries*, Academic Press, London, 1983, p. 169.
- 2 R. G. Burns and V. M. Burns, *2nd Int. Symp. on  $\text{MnO}_2$* , The Electrochemical Society, Tokyo, 1980, p. 97.
- 3 M. Voinov, *Electrochim. Acta*, 26 (1981) 1373.
- 4 G. Pistoia, *J. Electrochem. Soc.*, 129 (1982) 1861.
- 5 J. Vondrák, *Chem. Listy*, 73 (1979) 207.
- 6 J. E. B. Randles, *Discuss. Faraday Soc.*, 1 (1941) 11.
- 7 D. C. Grahame, *J. Electrochem. Soc.*, 99 (1952) C 370.
- 8 J. Vondrák, *Electrochim. Acta*, in press.
- 9 J. O. Besenhard and H. P. Fritz, *J. Electroanal. Chem.*, 53 (1974) 329.
- 10 J. O. Besenhard, *Carbon*, 14 (1976) 111.
- 11 H. Ikeda and S. Narukawa, *J. Power Sources*, 9 (1983) 329.
- 12 G. Pistoia, *J. Power Sources*, 9 (1983) 307.

- 13 S. Atlung, in A. Kozawa *et al.* (eds.), *Progress in Batteries and Solar Cells*, Vol. 2, JEC Press, Cleveland, 1979, p. 96.
- 14 S. Atlung, K. West and T. Jacobsen, in D. W. Murphy *et al.* (eds.), *Materials for Advanced Batteries*, Plenum Press, New York, 1981, p. 275.
- 15 J. O. Besenhard, J. Heydecke, E. Wudy and H. P. Fritz, *Solid State Ionics*, 8 (1983) 61.